Article

Investigating the Optimal DOD and Battery Technology for Hy-brid Energy Generation Models in Cement Industry Using HOMER Pro

Yasir Basheer [1], Saeed Mian Qaisar [2,3,*], Asad Waqar [4,*], Fahad Lateef [5], Ahmad Alzahrani [6,*]

1. Department of Electrical Engineering, Riphah International University, Islamabad 46000, Pakistan; yasir.basheer@riphah.edu.pk (Y.B.)
2. Electrical and Computer Engineering Department, Effat University, Jeddah, 22332, Saudi Arabia; (S.M.Q.)
3. Communication and Signal Processing Lab, Energy and Technology Center, Effat University, Jeddah 22332, Saudi Arabia; (S.M.Q.)
4. Department of Electrical Engineering, Bahria School of Engineering and Applied Sciences, Bahria University, Islamabad 44000, Pakistan; (A.W.)
5. Department of Computer Science University of Loralai, Pakistan; fahad.lateef@uoli.edu.pk (F.L.)
6. Electrical Engineering Department, College of Engineering, Najran University, Najran 11001, Saudi Arabia; (A.A.)

* Correspondence: sqaisar@effatuniversity.edu.sa (S.M.Q.); asadwaqar.buic@bahria.edu.pk (A.W.); asalzahrani@nu.edu.sa (A.A.)

Abstract Cement industry is one of the highest energy consuming industries. The quantity of fuel and energy needed accounts for most of the cost of cement manufacturing. Thermal power plants generate electricity but are harmful and ineffective by nature. As a backup mechanism to account for main grid failures, batteries can be utilized. In this paper the first ever investigation on battery's depth of discharge (DOD) for four different kinds of battery technologies is carried out in the framework of cement industry. The intended battery technologies are the lead-acid battery (LA), lithium-ion battery (Li-ion), vanadium redox battery (VR), and nickel–iron battery (Ni-Fe). Four hybrid energy generation models (HEGMs) for five cement plants of Pakistan using the HOMER pro software are proposed. Cement plants includes Askari Cement Plant, Wah (ACPW); Bestway Cement Plant, Kalar Kahar (BCPKK); Bestway Cement Plant, Farooqia (BCPF); Bestway Cement Plant, Hattar (BCPH); and DG Cement Plant, Chakwal (DGCPC). HEGM-1 comprises of a diesel generator (DGen), a photovoltaic system (PV), a converter, and a battery system. HEGM-2 comprises of a PV system, a converter, and a battery system. HEGM-3 is the grid-connected version of HEGM-1 and HEGM-4 is the grid-connected version of HEGM-2. A base-model consisting of grid only is used as a reference. A multi-criteria decision analysis (MCDA) is performed by formulating a cumulative objective function (COF) which includes net present cost (NPC), levelized cost of energy (LCOE), and greenhouse gas (GHG) emissions. The principal objective is the maximization of COF while simultaneously minimizing the objectives (NPC, LCOE and GHG emissions), based on optimal battery technology and DOD. The results reveal that VR is the most suitable battery technology with 10% DOD. It is achieved for DGCPC with HEGM-3 with 61.49% of NPC, 78.62% of LCOE and 84.00% of GHG emissions reduction as compared to the base model.

Keywords cement industry; depth of discharge; HOMER Pro Optimization; techno-economic analysis; net present cost; greenhouse gas emissions; levelized cost of electricity

 doi:10.20944/preprints202211.0222.v1

1. Introduction

As the world's population and industrialization grow, so does energy consumption. Between 2018 and 2050, it is anticipated that global energy consumption will rise by approximately 50%. The most significant source of energy has always been petroleum products, which have a negative impact on the environment. A specific battery ageing model with tentative verification for microgrid applications is still lacking, and one typical practice is to establish a fixed lifetime of 10 or 20 years [1]. Nonlinear functions of state of charge (SOC), depth of discharge (DOD), C-rate (defined as the charge or discharge current divided by the battery's capacity to hold an electrical charge, with the unit h1), temperature, and so on dictate battery ageing routes [2]. Nonetheless, the battery ageing models used in microgrid assessment and control references are primarily simplified to be linearly related to DOD and cycle quantities [3]–[5]. In [6] presents a feasible model for optimal scheduling with DOD and temperature parameters, neglecting C-rate and varying levels of SOC. In [7] researchers uses SOC and DOD limits to avoid sharp power changes from aggravating degradation while ignoring the quantitative impact of charge/discharge operations. The authors' in [8] provides a quadratic term to function battery degradation, such as film growth by current (the C-rate) but does not include a DOD factor. In [9] the study conducts a thorough analysis of domain-specific literature and proposes a weighted cost model that combines the results and parameters of mainstream studies; however, the distinct assumptions and experimental settings of those quoted models are not discussed in detail. Above all, developing an optimization-oriented battery SOH forecast model with experimental validation under microgrid settings is critical and still sought.

A lot of toxins are released into the air when petroleum products are burned, which is bad for human health and changes the environment because of ozone-depleting compounds [10]. By switching to cleaner energy sources, the issue of rising global surface temperatures could be addressed by lowering atmospheric carbon dioxide (CO2) levels [11]. Standalone hybrid energy system for cement industry of Pakistan is also discussed [12]. Renewable energy sources (RESs) that are good for the environment include hydropower, biomass, geothermal energy, solar photovoltaic (PV), and wind energy [13]. These RESs have the potential to offer everyone, regardless of where they live, clean energy that they can control. HESS are created by combining renewable energy sources (RESs) with conventional generators based on petroleum derivatives. As a result, they can address the issue of inconsistent and inconsistent RES supply. HESS frameworks that outperform single energy sources in terms of dependability, control, and value [14]. The most crucial factor in the implementation of HES factors may be their flawless planning and preparation. Each level of the microgrid can be improved to provide optimal operating conditions for all models. A framework plan may be revised to examine the best configurations for a single target capability or multiple objectives. Multi-objective advancement computers, on the other hand, are required when employing at least two target abilities. Increasing the framework's effectiveness and reducing its cost are two examples of such goals. Various strategies and procedures can be used to achieve the best possible plan of definite improvement issues [15]. A few tools for the coming new age include fluffy rationale, hereditary calculations, and molecule swarm enhancement. However, multiple cycles are carried out for conventional approaches, such as straight programming [16].

Some studies have specifically focused on how best to implement variant streamlining methods in HESs. To address the estimating streamlining problem of an isolated breeze/flowing/battery HES,[17] developed an advanced multi-objective evaluating improvement strategy based on Halton combination as well as the social rousing technique. The researchers noted that the enhanced computation and suggested method are effective in enhancing the system, and the efficient conditions of the framework are successful when coupled with the energy of the efficient approach. The researchers of [18] solved the HES assessment question for PV, wind, diesel, and batteries by employing inventive computing. In Saudi Arabia, a compelled little region is destroyed utilizing the proposed HES.

The results proved that the calculation was the best method for determining the best HES estimate. Hemeida and co. Using computational modeling and molecular swarm optimization, [19] in Libya, the most effective technique for a hybrid structured methodology was explored. An existing models with numerous goals proposed in [20] determines crossover systems between various source configurations. It was demonstrated that the crow calculation is more useful and effective than the molecular swarm advancement calculation. Experimental conclusions in everyday applications supported the framework's viability. In [21], HOMER was used to test whether a PV/biomass combination system that is both scientifically and cheaply viable could operate a remote location in Palestine. The creators believed that the proposed technology could cut down on pollution while also providing clean energy. Cao and others [22] The elephant crowding improvement calculation was used for multi-objective streamlining for a PV/wind/energy unit/battery HES. For the best design of a hybrid framework, it was concluded that the proposed approach is an efficient option. Using a metaheuristic grasshopper improvement computation, it was suggested that the best configuration of a HES composed of solar, wind, and batteries be investigated in order to supply energy to remote areas [23].The best method for measuring a PV, wind turbine, and battery edge design was determined using an energy channel calculation in [24].The designers discovered that, furthermore to meeting the essential limitations, utilizing the energy network estimation in conjunction with the recommended method is helpful for establishing the ideal economic plan for the HES.

To arrive at the ideal framework component estimates, it is necessary to carefully examine the availability of RESs, the appropriate control techniques, and the equipment of the framework [25]. To achieve the established objectives and guarantee safe operations, energy the board control frameworks are required. They are also required to allow numerous elements within a given framework to interact, join, and connect. The proper energy the board approach allows the system to focus on the load, lowering both energy expenses and ozone harmful element emissions while expanding the shares' lifespan to operate on the exhibition and suggest a long - term socio practical decision [26], [27]. When the RESs by itself can fulfill the demand, generator and battery dispatch management are used [28]. In HOMER programming, the two primary default dispatch methods are load following (LF) and cycle charging (CC). These methods select the highly possible design that can fulfill the power demand at every successive stage without concern the future demand shape or source characteristics. The generator behaves differently when the LF and CC dispatch techniques are used. The LF approach is used by the generator to meet the load needs without the battery being charged. During this technique, RESs are utilized to charge the battery. Because the generator is functioning at full capacity during the CC operation, it cannot access extra electricity [29].

Most of the test research has been focused on improving the HESs proposal in HOMER using both LF and CC approaches. According to [30], HOMER can effectively propose an off-background HRES for a regional order in India. From a financial standpoint, the inventors claim that the CC method performs better than the LF method. According to the investigation in [31], HES used the LF methodology and multicriteria planning to fulfill the energy demand in a countryside Tanzanian site. The findings showed that the recommended HES is a novel approach to billing the selected location. Elkadeem Ma and others [32] investigated whether a HES and a different assimilation de-salination plant could be combined to supply Egypt's international airport with water and electricity. The CC technique was utilized to ensure control of the flow among the elements. The findings confirmed the proposed HES's utility regards of information, resources, and cash. In Malawi, an effective paradigm for an examination involving a range of ages was investigated [33]. The analysis was carried out with the help of the LF and CC dispatch systems. Long-term research indicates that the most common configuration employs the LF technique. The system was analyzed in Nigeria [34] from the perception of financial and technical outrage. The energy flow between the components was controlled using the LF method. Based on the exploratory and comparative findings, it was concluded that the

proposed architecture is a feasible alternative for one's own lattice provincial jolt. Nesamalar and co. [35] provided a particular and an Indian learning facility's PV/diesel/battery HES's economic analysis by utilizing the LF and CC methodologies, both off-grid and on-grid. It was determined that the on-lattice HES with LF dispatch was the best option for the suggested location. The researchers investigated employing the LF and CC strategies to oversee the operation of a hybrid sustainable aging framework in Turkey. It was thought that the system using the CC method had lesser levelized cost of energy (LCOE) and net present cost (NPC) than the system using the LF method. In [36], the shudder of a region in Malawi was examined for an optimal HES strategy. The energy shift between the heap and the various components of the framework was examined using the CC approach. It has been demonstrated that the NPC suffers because of changes in fuel prices and wind speed over the course of the project. The framework's de-signers evaluated the technical, financial, and energy benefits of using a PV, diesel engine, and battery to supply electricity to a specific location in Minya City, Egypt, in [37]. According to the findings, the financial execution of the LF system is superior to that of the CC technique. A relationship of HESs in eight eco-friendly regions of Iran was finished using the CC strategy in [38]. It was thought that a lattice, PV, and wind turbine would make the ideal HES. In New Zealand, the LF method was used to investigate an independent breeze/flowing/diesel HES for the shock of coastal systems for strategy streamlining [39]. Corresponding to the findings, the ideal HES plan is put up to provide friendly scientific, economic, and organic implementation.

Hybrid frameworks have a lower NPC, researchers have demonstrated. In addition, the LCOE outperformed a single framework when it came to gathering required electrical demands [40], [41]. Hybrid energy frameworks regarding financial, ecological, and dependability have been the subject of a few studies [42], [43]. Panapakidis et al., in [44], have looked at the techno-economic reachability of four different hybrid power system that have been used for a long time to focus on the power concern of an off-grid home in different parts of Greece. The framework with the lowest absolute setup cost was selected as the benchmark for offering the best electric solution for networks, claims the study. Nandi et al. carried out a different analysis [45] looked at whether to use a combined energy system rather than a free generator for the local provincial jolt. In the evaluation, distinct monetary markets were considered, and the findings demonstrated that a combined energy structure has lower COE and NPC in comparison to an available diesel generator (DGen).

1.2 Research Gap

According to the literature, several studies have been conducted to evaluate the ideal design of various HEGM-based power systems in terms of economics and reliability. According to the studies, the battery, as an energy storage technology and battery depth of discharge (DOD), has played a significant role in the renewable generation-based power system. However, the data shows that only lead acid (LA) and lithium-ion (Li-ion) batteries have been typically employed in the studies. However, the studies on the employment of other battery technologies have been seen to be uncharted in HEGM based system to conduct economic studies on different battery DOD levels.

1.3 Contribution

- To design an optimal model of the standalone as well as grid connected HEGMs having with focus on battery technologies and DOD levels in cement industry of Pakistan
- To assess the performance of the proposed HEGMs based on load profiles of 5 cement industries and associated geographical resource data.
- A multi-criteria decision analysis (MCDA) is performed by formulating a cumulative objective function (COF) which includes the simultaneous minimization of NPC, LCOE, and greenhouse gas emissions (GHG emissions).

 doi:10.20944/preprints202211.0222.v1

- To perform the MCDA on the four different battery technologies including LA, Li-ion, vanadium redox (VR) and nickel-iron (Ni-Fe) in the proposed HEGMs.
- As per the authors' best of knowledge the proposed study which considers the minimization of NPC, LCOE and GHG emissions with focus on battery technologies and optimal DOD levels has not been investigated before in the cement industry of Pakistan.

In rest of the paper, the MCDA for HEGMs based on battery technologies is performed in four test cases:

Case-1: LA
Case-2: Li-ion
Case-3: VR
Case-4: Ni-Fe

Similarly, five cement plants are considered as test sites:

Cement Plant-1: Askari Cement Plant, Wah (ACPW).
Cement Plant-2: Bestway Cement Plant, Kalar Kahar (BCPKK).
Cement Plant-3: Bestway Cement Plant, Farooqia (BCPF).
Cement Plant-4: Bestway Cement Plant, Hattar (BCPH).
Cement Plant-5: DG Cement Plant, Chakwal (DGCPC).

2. Methodology

HEGMs were employed in the plan of this energy-producing system. The methodology of the study is presented in Figure 1.

- To strengthen the microgrid. The load profile, equipment data, and whether data like sun irradiance are among the inputs that Homer Pro requires.
- The selected resources will serve as the basis for the analysis. Techno-economic analyses are conducted at various DOD levels to ascertain the best preference in terms of NPC, LCOE, and GHG emission decrease.
- Using the enumerative optimization method, HOMER examines each combination that fails to meet the requirements, compiles the best options, and ranks them according to the considers factors.

2.1. Optimizaton problem

NREL created a tool for optimization called HOMER.HOMER employs a derivative-free optimizer. An improved grid search approach is used by the optimization algorithm. The optimal solution is chosen by HOMER after the user inputs a number of parameters [46]. The best option is ranked by HOMER based on the objective.

Using HOMER, reseachers can also relate the scientific and financial facets of various generator-storage unit combinations. By considering MCDA best result obtained based on the minimization of NPC, LCOE, and GHG emissions.

Preprints (www.preprints.org) | NOT PEER-REVIEWED | Posted: 11 November 2022 doi:10.20944/preprints202211.0222.v1

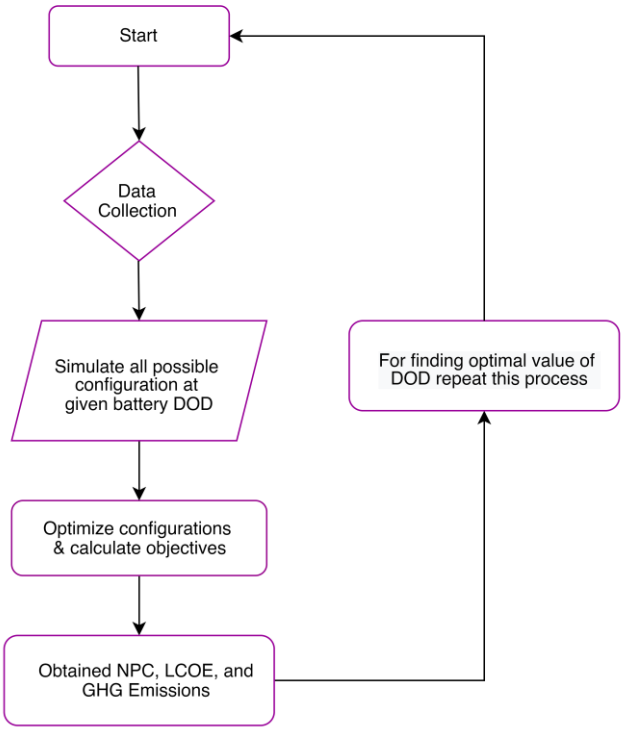

Figure 1. Methodology framework of the hybrid microgrid design

2.2. Objectives

Numerous factors influence the optimal configuration. Among the considered criteria are minimizing NPC, LCOE, and GHG emissions. Multi-criteria decision analysis is used to determine the ideal configuration of the microgrid. For this a cumulative objective function (COF) was considered as shown in Equation (1).

$$COF = [W_1(NPC) + W_2(LCOE) + W_3(GHG\ Emissions)] \quad (1)$$

Where, W_1 is 33.33%, W_2 is 33.34% and W_3 is 33.33%. As, the objective parameters have different units, so Equation (2) used to make these parameters unitless.

$$Normalize\_value = \frac{Base\,value - Actual\,value}{Base\,value} \quad (2)$$

Normalize_value is the unit less value, Basevalue is the value of base case considered in this study and Actualvalue is the value to be normalized. Equation (2) is utilized for each parameter independently, and the COF for each HEGM is calculated using Equation (1).

As Equation (2) illustrates, if Actualvalue exceeds Basevalue, Normalize_value becomes negative and also COF. Minimum COF results in maximum NPC, LCOE, and GHG emissions, and vice versa.

2.2.1. Net Present Cost

The numerous continuing cost combinations are comparable to the NPC that support experienced during its effective life, with a reduction of the improvement value at that

 doi:10.20944/preprints202211.0222.v1

point. The costs that are remembered for the net present cost are the costs that are shown in Equation (3) in accordance with reference [47] for initial expenditure, replacement cost, activity, and maintenance cost.

The total NPC is determined using the formula below:

$$C_{NPC} = \frac{C_{ann.tot}}{CRF\left(i.R_{proj}\right)} \quad (3)$$

Here, Cann, tot = Annualized cost. i = Interest rate (Annual). R_{proj} = Project lifetime. CRF (.) = Capital recovery factor.

2.2.2. Levelized Cost of Energy

The predetermined shaped framework delivers per KWh of energy. The Equation (4) from [47] is used by HOMER to determine the ideal COE for a standalone system.

$$LCOE = \frac{C_{ann.tot}}{E_{prim} + E_{def} + E_{grid.sales}} \quad (4)$$

E_{def} is the total deferrable load, E_{prim} is the entire primary load, Cann. tot is the yearly total cost, and $E_{grid,}$ sales is the quantity of energy supplied to the grid (per year).

2.2.3. GHG Emissions

Depending on the power resources employed, energy generation generates a variety of hazardous gas emissions. The amount of CO2 produced per kWh is dictated by the power resources used to generate the energy, and it fluctuates subject on the fuel utilized, which is why it differs every second. Furthermore, each kWh produces 1.34 g of nitrogen oxides and 2.74 g of carbon dioxide. Nitrogen oxides (NO), Sulphur dioxide (SO2), carbon monoxide (CO), unburned hydrocarbons (UHCs), and carbon dioxide (CO2) were not found in HEGM-2.

2.3. Hybrid Energy Generation Models Designing

For the techno-economic analysis, four HEGMs were developed using the Homer Pro software. A photovoltaic (PV), converters and a battery system, generators for top load needs are all part of the suggested system. The four types of HEGMs that have been developed for this study are listed below. These are the options that are provided for each HEGM that are the most cost-effective and sensible options. Each HEGM has its own gains and limits to meet the necessary load requirements.

2.3.1. PV

The standard flat-plate photovoltaic is utilized in the manufactured variations.Generic PV panels have an efficiency of 14% and a lifespan of 25 years.Under normal operating conditions, the module's output power is calculated using Equation (5) [48].

$$P_{pv} = f_{pv} \times Y_{pv} \times \frac{I_T}{I_S} \quad (5)$$

Ppv is the abbreviation for the PV panels' meagre power output in kW. The term "total incident radiation" (measured in kWh/m2) as IT. IS = 1000 W/m2; The reduction factor, also known as f_{pv}, is determined by factors such as energy loss caused by splices and long wiring distances.

 doi:10.20944/preprints202211.0222.v1

2.3.2. Battery Storage System

Four different kinds of batteries, including the Hoppecke 24 OPzS 3000-Vented lead-acid **(Case-1)**, the Blue Ion 2.0 lithium-ion battery **(Case-2)**, the redT vanadium redox battery **(Case-3)**, and the Iron Edison nickel–iron battery **(Case-4)**, were put through tests to see which one is best suited for use in hybrid systems. Equation (6) [49] depicts the DOD expression, and Table 3 contains important information about the chosen batteries.

$$DOD(\%) = 100\left[\frac{1}{Q}\int_{0}^{1} i(t)\,dt\right] \quad (6)$$

The depth of discharge is calculated by dividing the maximum battery capacity (Q) by the load current (i(t)).

Contrary to the DOD, SOC can be related to: "DOD = 1 – SOC".

Table-1: Specifications of induced batteries [50]

Parameters	**Case-1**	**Case-2**	**Case-3**	**Case-4**
Nominal voltage (V)	2	51.2	48	1.2
Max. capacity (Ah)	3570	328	417	1000
Nominal capacity (kWh)	7.15	16.8	20	1.2
Max. charge current (A)	610	263	105	500
Max. discharge current (A)	610	328	105	500
Roundtrip efficiency (%)	86	97	75	85
Capital cost ($)	722	15,000	10,700	970
Replacement cost ($)	665	13,800	9,300	890
O&M cost ($/year)	180	1	1	1
Lifetime (years)	15	25	25	20
Nominal voltage (V)	2	51.2	48	1.2

2.3.3. Converter

These HEGMs are used with the Homer pro software's generic system converter. It has rectifier and inverter modes of operation. When neither solar nor wind power is available, the converter only works in inverter mode; This typically takes place at night and when the sky is cloudy. When sufficient renewable energy is available to charge the battery system, the converter only uses its rectifier mode. The converter has an efficiency rating of 95%.

The effectiveness and selection of the inverter (Pl, s (t)) determine the power converter's maximum capacity for converting DC to AC. In [51], it is expressed as Equation (7):

$$P_{l,s}(t) = P_{input}(t) * \eta_{conv} \quad (7)$$

where $P_{input}(t)$ stands for the converter's input power and η_{conv} for its efficiency.

2.3.4. Diesel Generator

A standard small-size generator is used in the design and simulation processes in HEGM-1 and 3. The generator is adapted to meet its requirements by the Homer Pro program. A connection between the rated power of a diesel generator (DGen) and its output can be seen in Equation (8) from [52]. Table 2 contains the cost of components used in this study.

Preprints (www.preprints.org) | NOT PEER-REVIEWED | Posted: 11 November 2022 doi:10.20944/preprints202211.0222.v1

Table 2. Components cost [53]

Components	Initial cost US$/kW	Replacement cost US$/kW	Operating cost	Lifetime in years
PV	350	350	10	25
DGen	400	400	0.010	15,000 h
Converter	300	300	0.00	15

$$PGD = \eta diesel \times NDG \times PGD, N \quad (8)$$

where NDG is the total number of identical diesel generators, PDG is the combined output of the generators, and η is the generator's productivity.

2.3.5 Grid

Using conventional grid power, the electricity is brought to the site. When renewable sources are unable to meet the demands of the load, the AC power is supplied to a designated plant, which will serve as a backup source of power for the load. Utilizing net metering (NM), the integrated grid system will also be beneficial for obtaining surplus power from proposed HEGMs. A billing mechanism that allows a customer to sell surplus electrical power into the grid and adjust the credit amount by drawing power from the grid is what the NM approach encourages power consumers to use for cost-effective power generation renewable sources. In addition, NM serves as a regulatory incentive that enables a variety of small and medium-sized consumers to acquire credits for excessive electricity generation. In contrast, customers in developed nations who generate electricity from renewable energy sources receive a fiscal incentive known as a feed in tariff (FIT). Each year, the energy provider receives payment in the form of a fixed unit price for the electricity it generates. As a result, NEPRA's commercial electricity price for off-peak hours has been used to calculate the proposed system's unit price with NM at 0.250 $/kWh [54].

HEGM Configurations

- Figure 2 shows HEGM-1. it will have a PV, DG, converter, and battery.

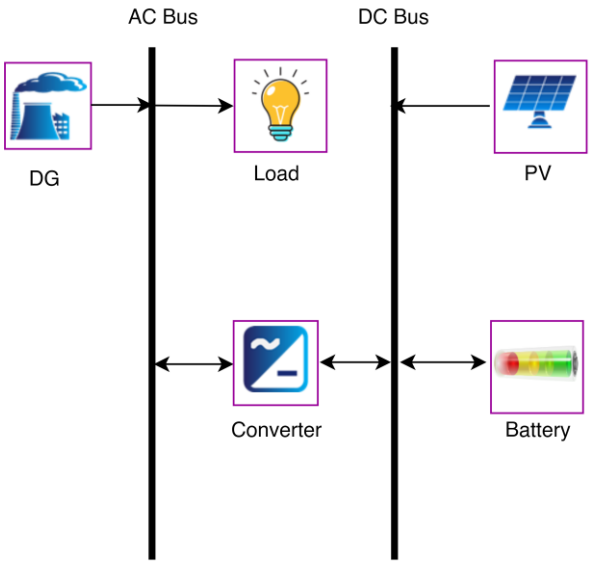

Figure 2. Schematic diagram of HEGM-1

- Figure 3 shows HEGM-2., it will only PV, converter, and battery.

Preprints (www.preprints.org) | NOT PEER-REVIEWED | Posted: 11 November 2022 doi:10.20944/preprints202211.0222.v1

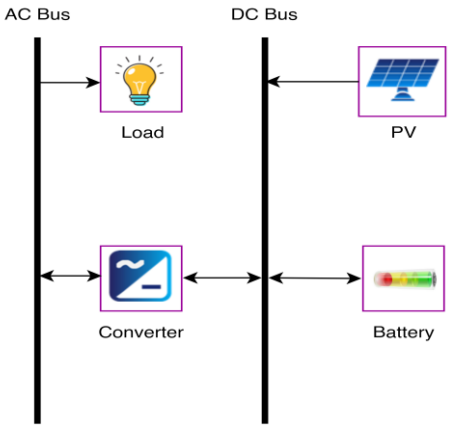

Figure 3. Schematic diagram of HEGM-2

- Figure 4 shows the HEGM-3, it will have a grid-connected PV, DG, converter, and battery.

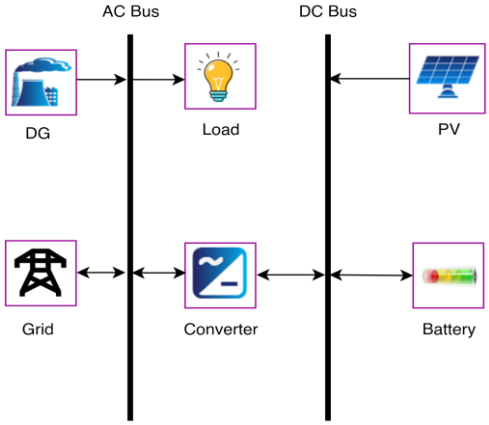

Figure 4. Schematic diagram of HEGM-3

- Figure 5 shows HEGM-4, it will grid-connected PV, converter, and battery.

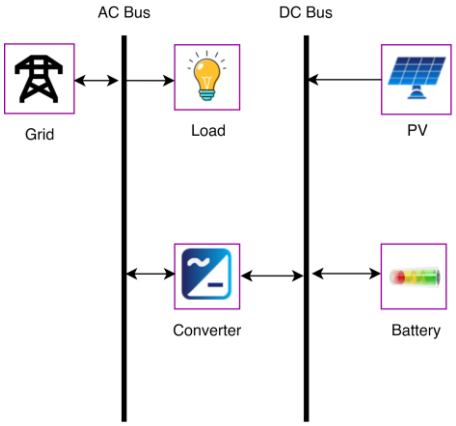

Figure 5. Schematic diagram of HEGM-4

- Figure 6 shows Base-Model, it has only grid and act as base case in this study

Preprints (www.preprints.org) | NOT PEER-REVIEWED | Posted: 11 November 2022 doi:10.20944/preprints202211.0222.v1

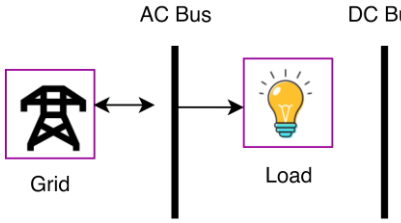

Figure 6. Schematic diagram of Base-Model

2.4. Site Area

The cement plants are located in Pakistan, and their coordinates are as follows:

ACPW**:** 33.8170° N, 72.7238° E
BCPKK: 32.7185° N, 72.7761° E
BCPF: 33.8282° N, 72.8337° E
BCPH: 33.8481° N, 72.8679° E
DGCPC: 32.7344° N, 72.8100° E

Figure 7 represents the locations of the cement manufacturing facilities.

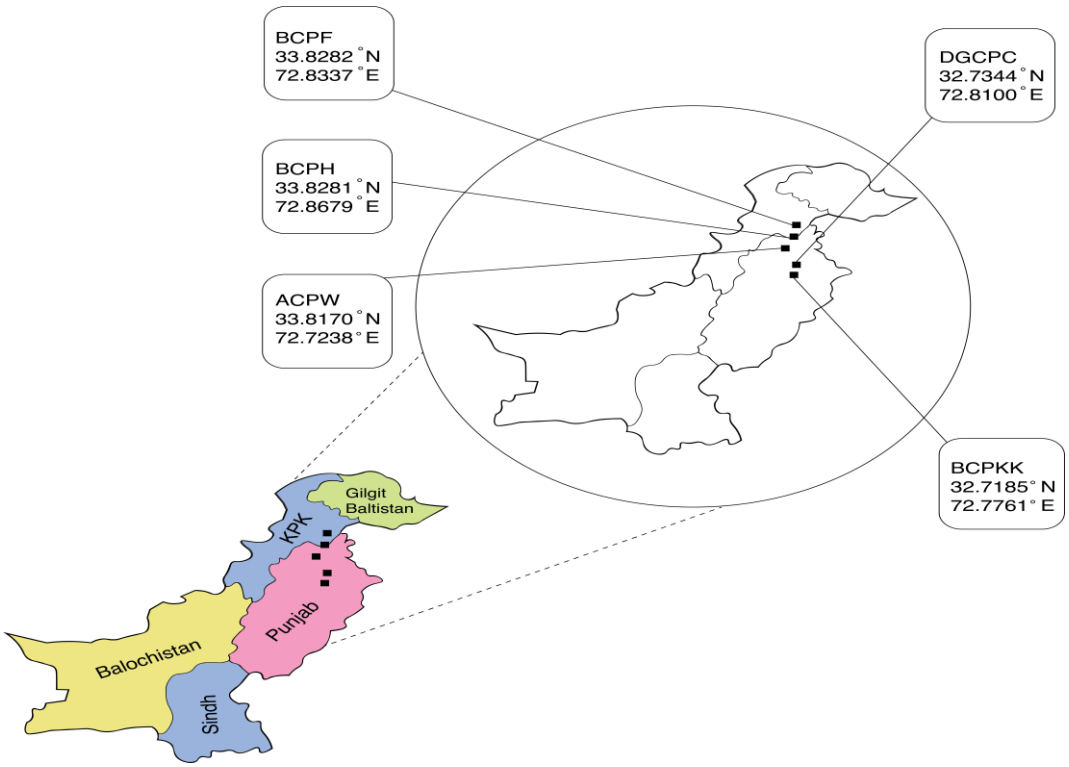

Figure 7. The geographical locations of cement plants

2.4.1. Load Profile

The load profile for five cement industries: For ACPW, is 18MW. BCPKK, BCPF, and BCPH's average demands are 34, 37, and 18 MW, accordingly. The average load for DGPC is 31 MW. In Figure 8 energy utilized per day is shown from [12].

Preprints (www.preprints.org) | NOT PEER-REVIEWED | Posted: 11 November 2022 doi:10.20944/preprints202211.0222.v1

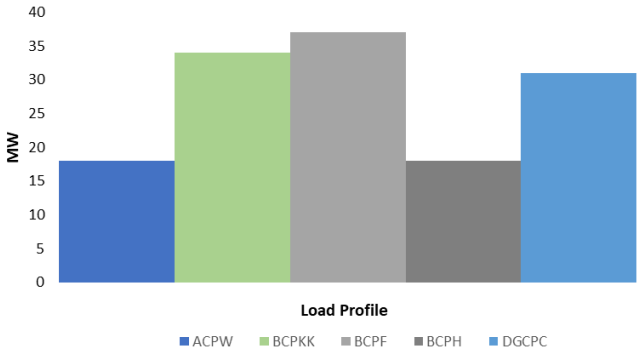

Figure 8. Daily load profile of the Plants

2.4.2. Energy Resource Assessment

The location of the area has a significant potential for energy resources. In Pakistan, there are a lot of data about the potential of solar power. When determining their resource potential, the prospective locations' geographical location has been taken into consideration.

The places that were chosen for the have a lot of potential for sun-oriented travel. Figure 9 provides an overview of the facilities under consideration's annual ambient temperatures. It demonstrates that the ACPW is 22.85 °C. The annual average ambient temperature for BCPKK is 17.80 C°. The annual average ambient temperature for BCPF is 22.75 C°. The annual average ambient temperature for BCPH is 22.75 C°. The annual average ambient temperature for DGCPC is 24.21 C°. ACPW's annual definite photovoltaic power yield is 1620 kWh/kWp. The explicit photovoltaic power output for BCPKK is 1631 kWh/kWp. While the PV output for BCPF and BCPH is 1621 kWh/kWp. It will be 1651 kWh/kWp for DGCPC.

The annual daily radiation levels are depicted in kWh/m2 in Figure 10. The ACPW and BCPKK have annual average values of around 4.91 kWh/m2/day, the BCPF and BCPH have values of 4.89 kWh/m2/day, and the DGCPC has values of 5.027 kWh/m2/day. The development of solar-powered chargers is anticipated due to Pakistan's average daily solar radiation of 5.0 kWh/m2/day. Sun-radiation data can be estimated using the available number of web-based data sets. World-weather-online, a NASA website, and a book of sun-radiation-oriented maps served as sources for these data [55].

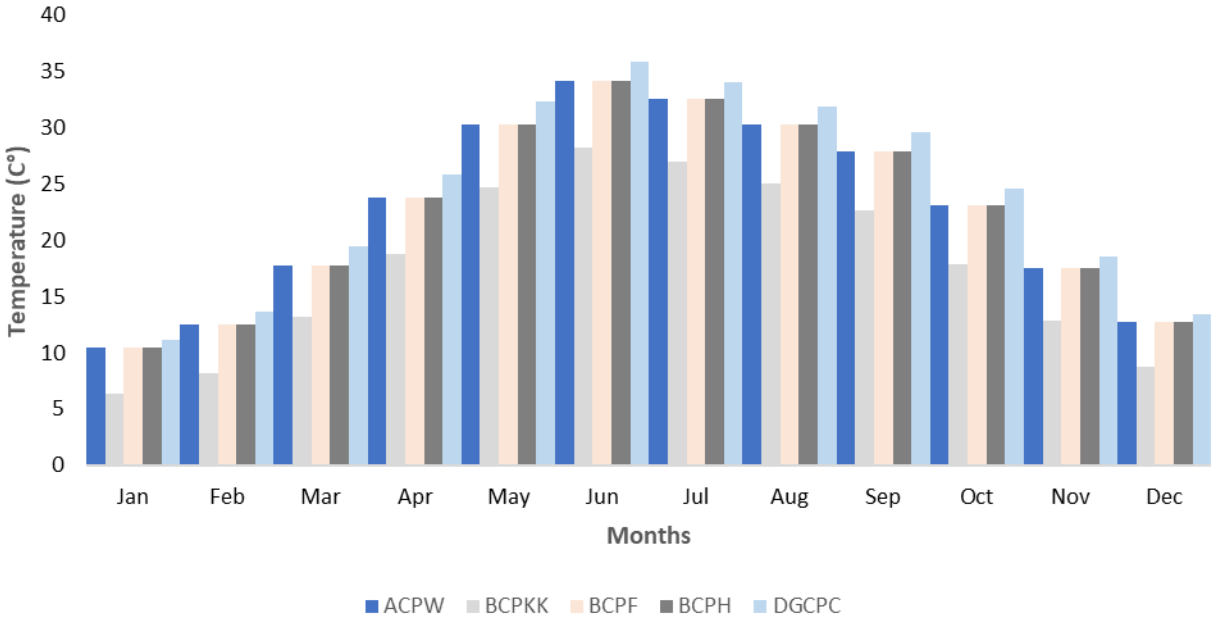

Figure 10. Ambient Temperature of the plants

Preprints (www.preprints.org) | NOT PEER-REVIEWED | Posted: 11 November 2022 doi:10.20944/preprints202211.0222.v1

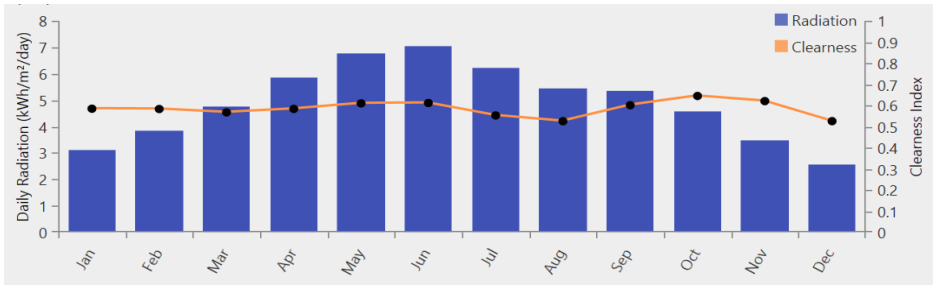

(a) ACPW

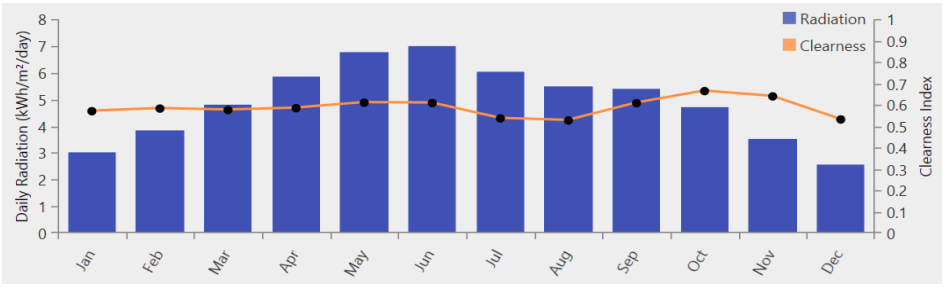

(b) BCPKK

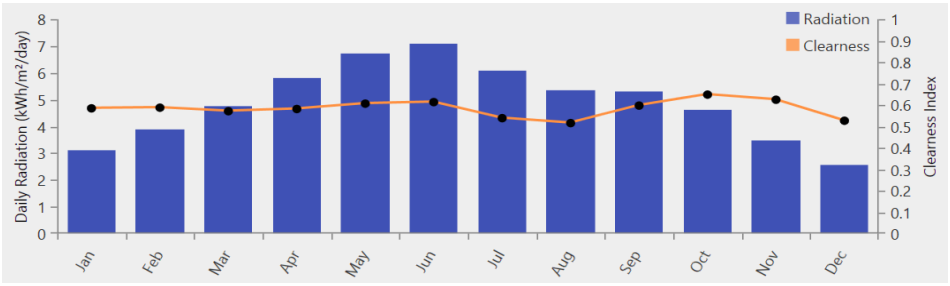

(c) BCPF

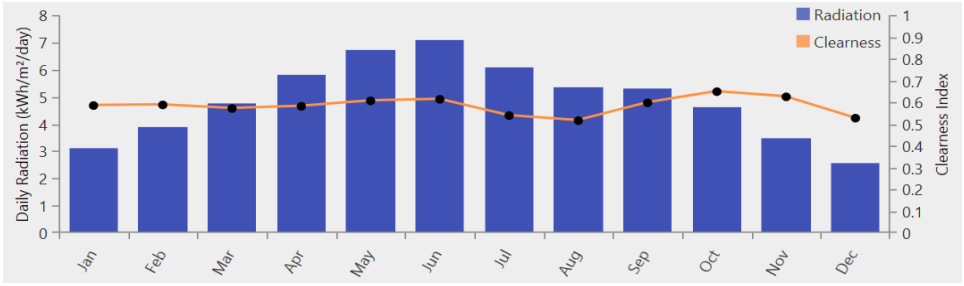

(d) BCPH

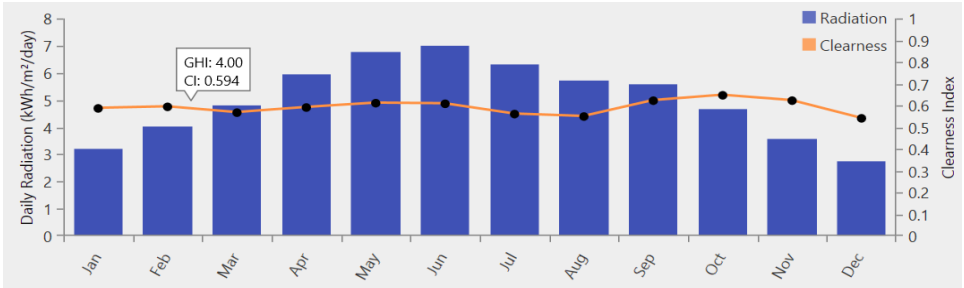

(e) DGCPC

Figure 10. Annual daily radiation and clearness index

Preprints (www.preprints.org) | NOT PEER-REVIEWED | Posted: 11 November 2022 doi:10.20944/preprints202211.0222.v1

3. Results

The analysis was performed on Homer Pro software using the NPC, LCOE and GHG emissions mentioned previously in this section to discover the most efficient solution. The output was customized by considering the COF. By doing so, authors scale down the system's result for better understanding.

Base-Model results shows in Table 3.

Table 3. Base-Model Objective parameters.

	ACPW	BCPKK	BCPF	BCPH	DGCPC
NPC ($)	519,571,900	981,413,600	1,068,009,000	519,571,900	894,818,300
LCOE ($/KWh)	0.24	0.24	0.24	0.24	0.24
GHG Emissions (Kg/year)	100,297,094	189,450,068	206,166,250	100,297,094	172,733,884

3.1 Case-1 (LA)

Table 4-8 shows the result of cumulative objective function. From the table each HEGM has different values on different DOD levels. Maximum COF has the least value of NPC, LCOE, GHG Emissions for Case-1.

Table 4. COF of ACPW Case-1

DOD	95 %	90 %	80 %	70 %	60 %	50 %	40 %	30 %	20 %	10 %
HEGM-1	8.309048	8.316613	8.325030	8.340154	8.359099	8.244080	8.296404	8.423305	8.450984	8.387312
HEGM-2			.323841	2.327906	1.455369	4.364195	7.379507	8.351989	8.700067	
HEGM-3	0.252289	9.306461	9.338111	9.364419	0.214309	9.420816	9.416356	0.393795	0.399282	9.490151
HEGM-4	0.448667	0.459096	0.997710	1.380279	1.637904	1.499927	1.953091	1.772267	1.677465	1.811165

Table 5. COF of BCPKK Case-1

DOD	95 %	90 %	80 %	70 %	60 %	50 %	40 %	30 %	20 %	10 %
HEGM-1	8.413604	8.421139	8.427800	8.467225	8.461549	8.480286	8.614947	8.525237	8.576876	8.682644
HEGM-2					.387551	9.791954	4.185230	5.984204	7.489451	8.136725
HEGM-3	0.024743	0.691159	0.488904	0.993303	0.855906	0.884805	1.186039	0.285777	1.363819	0.701490
HEGM-4	8.116612	7.828845	5.888772	6.759302	0.337366	9.351201	0.167735	0.176713	0.585406	0.330276

Table 6. COF of BCPF Case-1

DOD	95 %	90 %	80 %	70 %	60 %	50 %	40 %	30 %	20 %	10 %
HEGM-1	8.307484	8.315045	8.337677	8.242988	8.261850	8.280708	8.381242	8.329603	8.283627	8.310384
HEGM-2				.252383	2.328402	1.455845	4.727758	7.592530	8.352870	8.701072
HEGM-3	0.532785	0.529518	0.552000	0.912183	0.496744	0.529106	0.648524	0.652861	0.634324	0.705513
HEGM-4	7.978700	6.410620	7.683328	6.772288	8.726518	7.523192	7.586701	7.572925	7.588073	7.600691

Table 7. COF of BCPH Case-1

DOD	95 %	90 %	80 %	70 %	60 %	50 %	40 %	30 %	20 %	10 %
HEGM-1	8.136315	8.143876	8.166540	8.181662	8.200567	8.219463	8.355451	8.357980	8.384874	8.439757
HEGM-2				.459818	2.652826	1.452785	4.680924	7.589581	8.350390	8.698619
HEGM-3	0.867992	0.880244	0.880986	7.255703	0.934263	0.952079	7.618859	0.984418	1.348956	8.535193
HEGM-4	0.506232	0.516661	0.867820	1.150001	0.497224	0.918137	1.482948	1.516784	9.729428	1.847558

Preprints (www.preprints.org) | NOT PEER-REVIEWED | Posted: 11 November 2022 doi:10.20944/preprints202211.0222.v1

Table 8. COF of DGCPC Case-1

DOD	95 %	90 %	80 %	70 %	60 %	50 %	40 %	30 %	20 %	10 %
HEGM-1	9.019604	9.027185	9.049998	9.155357	9.084062	9.102972	9.125666	9.152157	9.179661	9.202862
HEGM-2				.185653	4.094679	3.365139	7.161453	9.690471	0.450671	0.869763
HEGM-3	1.361494	1.373918	1.391115	1.763917	1.435483	2.213588	1.476197	1.489661	1.499318	2.262228
HEGM-4	9.277052	9.394307	9.608421	0.840389	0.948671	1.342487	1.477556	1.506377	1.851898	1.512699

"-" shows in table represent not feasible solution

3.2 Case-2 (Li-ion)

Table 9-13 shows the result of cumulative objective function. From the table each HEGM has different values on different DOD levels. Maximum COF has the least value of NPC, LCOE, GHG Emissions for Case-2.

Table 9. COF of ACPW Case-2

DOD	95 %	90 %	80 %	70 %	60 %	50 %	40 %	30 %	20 %	10 %
HEGM-1	3.590602	3.601841	3.620747	3.639661	3.721900	3.740813	3.759711	3.749231	3.771738	3.786962
HEGM-2						.12549598	.5860048	0.023192	1.39035	2.123872
HEGM-3	8.366916	8.366966	8.367064	8.367155	8.367252	8.367350	8.367443	8.367541	8.367631	8.367729
HEGM-4	0.963837	3.646341	3.936369	0.995541	1.128097	1.141819	1.156950	1.465572	1.479764	1.994354

Table 10. COF of BCPKK Case-2

DOD	95 %	90 %	80 %	70 %	60 %	50 %	40 %	30 %	20 %	10 %
HEGM-1	3.898835	3.910027	3.928868	3.947696	3.966526	3.985368	4.004195	4.023036	4.045423	4.067897
HEGM-2	93.509426	27.120920	14.348746	10.153935	5.018420	2 .433403	6.069172	8.015552	9.532135	11.082000
HEGM-3	6.307059	6.307114	6.307223	6.307335	6.307446	6.307554	6.307668	6.307778	6.307887	6.307996
HEGM-4	0.693909	1.794316	0.717358	1.991033	1.182362	1.196926	1.213634	1.440778	1.455775	3.141776

Table 11. COF of BCPF Case-2

DOD	95 %	90 %	80 %	70 %	60 %	50 %	40 %	30 %	20 %	10 %
HEGM-1	3.687925	3.699105	3.717918	3.736714	3.755530	3.774330	3.793143	3.811959	3.834308	3.856764
HEGM-2	89.520983	23.271483	11.226816	4.255683	1.745642	3.126632	7.586208	10.340363	1.391315	2.124240
HEGM-3	6.457935	6.457992	6.458102	6.458214	6.458325	6.458437	6.458548	6.458657	6.458771	6.458884
HEGM-4	9.674847	0.216074	9.697842	1.147145	1.204181	1.087272	1.102149	1.117320	1.129524	1.146864

Table 12. COF of BCPH Case-2

DOD	95 %	90 %	80 %	70 %	60 %	50 %	40 %	30 %	20 %	10 %
HEGM-1	3.623353	3.634580	3.653458	3.672323	3.768016	3.786909	3.805815	3.756233	3.776087	3.801397
HEGM-2						.125829	.880515	0.328382	1.390613	2.124122
HEGM-3	7.899395	7.899446	7.899548	7.899651	7.899753	7.899854	7.899956	7.900059	7.900161	7.900262
HEGM-4	3.920604	4.118072	3.944980	1.778792	0.446447	0.757425	0.474941	0.784490	0.798462	0.809963

Table 13 COF of DGCPC Case-2

DOD	95 %	90 %	80 %	70 %	60 %	50 %	40 %	30 %	20 %	10 %
HEGM-1	4.818228	4.859959	4.879190	4.898442	4.917677	4.936928	4.956163	4.994128	4.861206	5.006858

Preprints (www.preprints.org) | NOT PEER-REVIEWED | Posted: 11 November 2022 doi:10.20944/preprints202211.0222.v1

HEGM-2					.711659	.038630	.259313	1.313977	3.415306	6.701832
HEGM-3	6.926260	6.926313	6.926412	6.926512	6.926611	6.926711	6.926809	6.926910	6.927012	6.927112
HEGM-4	2.250202	1.7947959	2.4666338	2.8797861	9.6419307	7.7886583	8.9960397	2.0482479	3.0032288	3.66306

"**-**" shows in table represent not feasible solution

3.3 Case-3 (VR)

Table 14-18 shows the result of cumulative objective function. From the table each HEGM has different values on different DOD levels. Maximum COF has the least value of NPC, LCOE, GHG Emissions for Case-3.

Table 14. COF of ACPW Case-3

DOD	**95 %**	**90 %**	**80 %**	**70 %**	**60 %**	**50 %**	**40 %**	**30 %**	**20 %**	**10 %**
HEGM-1	3.067009	3.212975	3.233044	3.253121	3.100636	3.120422	3.088908	3.112343	3.201448	3.369229
HEGM-2				.257585	2.909738	9.327440	4.070659	4.768390	6.498461	7.021240
HEGM-3	3.588215	3.549502	2.985962	3.597755	3.626939	3.639366	3.658400	3.193252	3.108122	3.174249
HEGM-4	1.530972	9.967002	1.560669	0.559078	3.910336	3.889107	4.305445	4.506776	4.523130	4.355230

Table 15. COF of BCPKK Case-3

DOD	**95 %**	**90 %**	**80 %**	**70 %**	**60 %**	**50 %**	**40 %**	**30 %**	**20 %**	**10 %**
HEGM-1	3.182108	3.193742	3.213356	3.232981	3.252596	3.272224	3.415410	3.431580	3.455601	3.470725
HEGM-2					.188560	8.445984	0.725748	1.877953	4.517671	6.179258
HEGM-3	3.404185	3.412813	3.437756	3.460416	3.484545	3.508051	3.527200	3.550684	3.562451	3.755313
HEGM-4	0.540869	1.618390	5.232508	7.506233	5.792367	5.806909	4.935832	5.192847	5.571662	8.047148

Table 16. COF of BCPF Case-3

	95 %	**90 %**	**80 %**	**70 %**	**60 %**	**50 %**	**40 %**	**30 %**	**20 %**	**10 %**
HEGM-1	3.238125	3.249987	3.270015	3.290026	3.310051	3.330079	3.350108	3.373836	3.402203	3.425963
HEGM-2				.182673	2.909326	9.441800	4.071308	4.825432	6.499471	6.290012
HEGM-3	2.405479	2.414299	2.445241	2.471367	2.451014	2.442218	2.514775	2.466637	2.563919	2.478532
HEGM-4	0.477888	0.479708	0.483343	9.681027	9.684423	9.687833	0.606420	0.784108	1.107725	0.638366

Table 17. COF of BCPH Case-3

DOD	**95 %**	**90 %**	**80 %**	**70 %**	**60 %**	**50 %**	**40 %**	**30 %**	**20 %**	**10 %**
HEGM-1	3.060441	3.072177	3.091914	3.111638	3.167766	3.187533	3.339474	3.230788	3.198844	3.415849
HEGM-2				.541251	1.032910	0.189176	2.617731	4.824861	6.499169	6.289738
HEGM-3	3.118983	3.127610	3.253930	3.271375	3.300686	3.313859	3.342852	3.361662	3.279720	3.393698
HEGM-4	0.150264	8.614046	0.152519	2.697357	4.075350	3.198012	4.093743	4.329120	4.559990	4.579019

Table 18. COF of DGCPC Case-3

DOD	**95 %**	**90 %**	**80 %**	**70 %**	**60 %**	**50 %**	**40 %**	**30 %**	**20 %**	**10 %**
HEGM-1	5.068073	5.075124	5.096490	5.114219	5.131957	5.149690	5.167423	5.185171	5.256105	5.264442
HEGM-2				.335364	5.657591	2.372353	5.897303	4.365087	8.044211	8.263433
HEGM-3	4.517062	4.526180	4.545766	4.575288	4.593879	4.624056	4.637634	4.658769	4.667815	4.698037
HEGM-4	8.036022	7.963109	8.624074	9.232326	9.550136	0.162127	0.324192	0.339813	0.779757	2.775196

"**-**" shows in table represent not feasible solution

 doi:10.20944/preprints202211.0222.v1

3.4 Case-4 (Ni-Fe)

Table 19-23 shows the result of cumulative objective function. From the table each HEGM has different values on different DOD levels. Maximum COF has the least value of NPC, LCOE, GHG Emissions for Case-4.

Table 19. COF of ACPW Case-4

DOD	95 %	90 %	80 %	70 %	60 %	50 %	40 %	30 %	20 %	10 %
HEGM-1	4.128029	4.135122	4.156603	4.174450	4.192284	4.210124	4.227970	4.245811	4.279855	4.302198
HEGM-2						.433845	1.320295	2.865672	3.913544	6.762049
HEGM-3	4.758333	4.758661	4.759322	4.896629	4.760640	4.761300	9.275970	9.276202	9.276441	9.276680
HEGM-4	0.413315	9.453784	8.655046	0.723494	0.909694	0.725205	3.323595	1.552743	1.515132	1.512737

Table 20. COF of BCPKK Case-4

DOD	95 %	90 %	80 %	70 %	60 %	50 %	40 %	30 %	20 %	10 %
HEGM-1	4.4607051	4.4678315	4.4892828	4.5071259	4.4588395	4.4767197	4.5091615	4.6480081	4.5199295	4.6918407
HEGM-2						.244651	0.649540	2.424800	4.656390	5.319626
HEGM-3	6.993746	6.788941	6.789151	6.789364	6.789577	6.789786	6.625553	6.625751	6.625952	6.626150
HEGM-4	4.921911	4.929212	5.576436	6.464381	5.629950	5.661680	5.661680	5.661680	5.661680	8.928710

Table 21. COF of BCPF Case-4

DOD	95 %	90 %	80 %	70 %	60 %	50 %	40 %	30 %	20 %	10 %
HEGM-1	4.355447	4.362625	4.384221	4.402191	4.420175	4.438145	4.456132	4.474105	4.440365	4.443828
HEGM-2						.761097	1.222125	3.106206	4.173710	6.763261
HEGM-3	6.279386	6.279480	6.279677	6.279875	6.280071	6.280266	6.266289	6.266495	6.266697	6.266902
HEGM-4	6.906393	6.912989	7.003142	6.438905	7.776013	8.391286	8.394172	8.294910	8.308673	8.424548

Table 22. COF of BCPH Case-4

DOD	95 %	90 %	80 %	70 %	60 %	50 %	40 %	30 %	20 %	10 %
HEGM-1	4.111228	4.118375	4.139950	4.157885	4.175834	4.187798	4.211724	4.351259	4.376517	4.403374
HEGM-2						.014957	1.043574	3.104697	4.348961	6.761602
HEGM-3	4.844179	4.844538	4.845254	4.845965	4.846683	4.847394	9.172310	9.172524	9.172742	9.172962
HEGM-4	0.410242	9.393826	9.901701	0.704715	1.452831	1.465512	9.954940	1.578902	1.502824	1.500366

Table 23. COF of DGCPC Case-4

DOD	95 %	90 %	80 %	70 %	60 %	50 %	40 %	30 %	20 %	10 %
HEGM-1	5.068073	5.075124	5.096490	5.114219	5.131957	5.149690	5.167423	5.185171	5.256105	5.264442
HEGM-2					.300604	.786439	4.291846	6.401341	8.053145	8.554656
HEGM-3	7.810614	7.810721	7.810933	7.811140	7.811353	7.811561	7.078553	7.078752	7.078953	7.079150
HEGM-4	6.504811	6.230492	6.852890	5.582855	6.235738	6.206691	5.048762	3.344564	6.298462	6.386623

"**-**" shows in table represent not feasible solution

3.5 Graphical Representation

For the Tables 4-23 HEGM-3 is the most optimal model in each Figure 11 shows the Graphical representation of optimal case and optimal DOD for each selected plant. Table 24 shows the comparison of optimal solution with the base model.

Preprints (www.preprints.org) | NOT PEER-REVIEWED | Posted: 11 November 2022 doi:10.20944/preprints202211.0222.v1

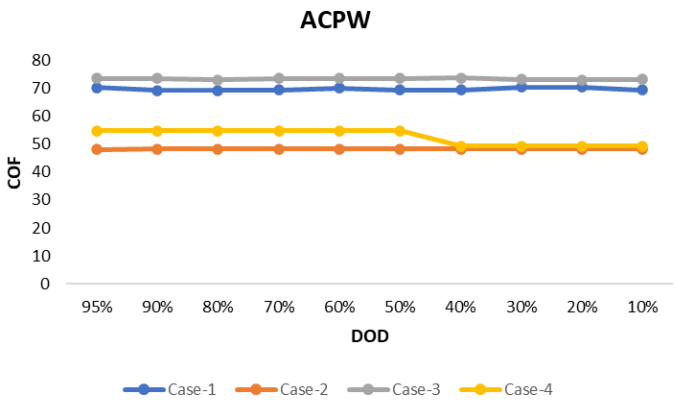

(a)

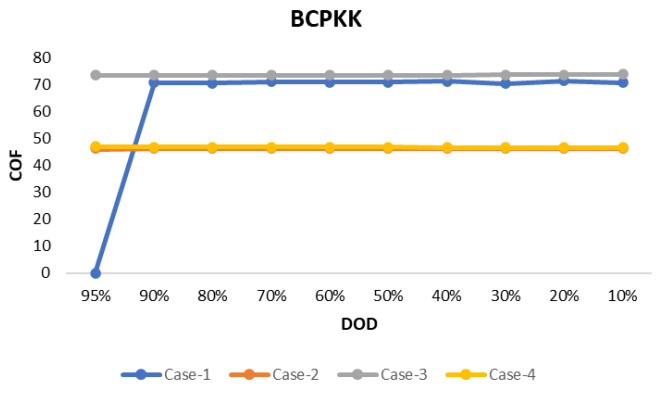

(b)

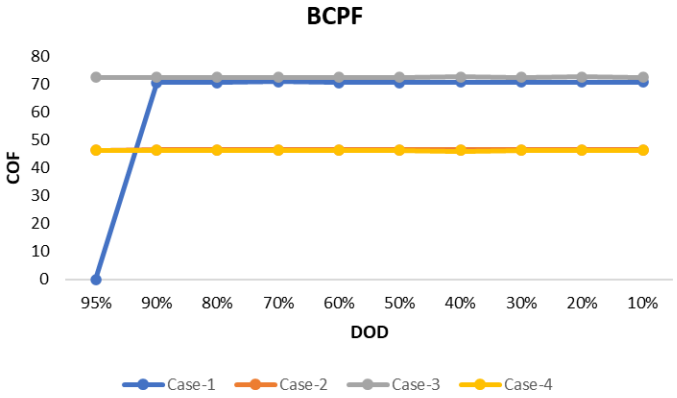

(b)

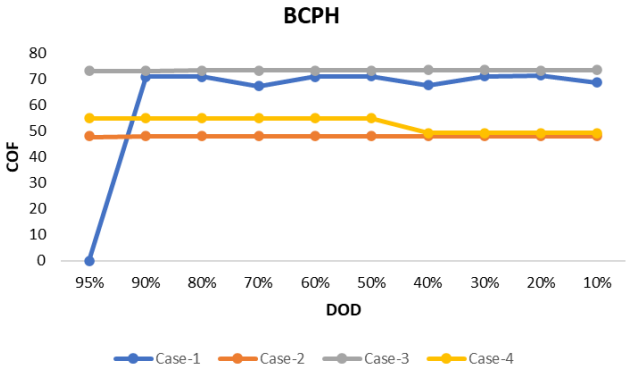

(d)

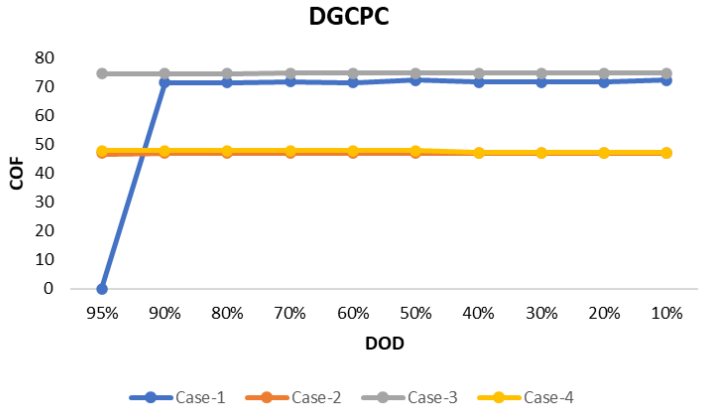

(e)

Figure 11. Optimal DOD and battery type for each plant

Table 24. Comparison of optimal solutions from base model

		NPC ($)	LCOE ($/kwh)	GHG emissions(kg/year)
	Base-Model	519,571,900	0.24	100,297,094
ACPW	Optimal solution	205,501,300	0.0530640	17,392,196
	Reduction (%)	60.45	77.89	82.66
	Base-Model	981,413,600	0.24	189,450,068
BCPKK	Optimal solution	390,028,000	0.05294655	32,034,909
	Reduction (%)	60.26	77.94	83.09
	Base-Model	1,068,009,000	0.24	206,166,250
BCPF	Optimal solution	430,640,400	0.0546779	39,547,271
	Reduction (%)	59.68	77.22	80.82
	Base-Model	519,571,900	0.24	100,297,094
BCPH	Optimal solution	205,355,000	0.0533465	18,098,903
	Reduction (%)	60.48	77.77	81.95
	Base-Model	894,818,300	0.24	172,733,884
DGCPC	Optimal solution	344,564,100	0.0513028	27,638,652
	Reduction (%)	61.49	78.62	84.00

4. Discussion

For ACPW when battery discharge from 10% to 95% COF varies from 3.12549598 to 73.658400 and the most optimal solution is HEGM-3 for Case-3 having NPC of USD 205,501,300, LCOE USD 0.0530640/kwh and GHG Emissions is 17,392,196 kg/year at the optimal DOD of 40%.

For BCPKK when battery discharge from 10% to 95% COF varies from 1.244651 to 73.755313 so the most optimal solution is HEGM-3 for Case-3 having NPC of USD 390,028,000, LCOE USD 0.05294655/kwh and GHG Emissions are 32,034,909 kg/year at the optimal DOD of 10%.

In case of BCPF COF varies from 3.125829 to 73.393698 and optimal solution is HEGM-3 for Case-3 with USD 430,640,400 NPC, LCOE is USD 0.0546779/kwh and GHG emissions are 39,547,271 kg/year at the optimal DOD of 20%.

In case of BCPH COF varies from 3.252383 to 72.563919 and optimal solution is HEGM-3 for Case-3 with USD 205,355,000 NPC, LCOE is USD 0.0533465/kwh and GHG emissions are 18,098,903 kg/year at the optimal DOD of 10%

In case of DGCPC COF varies from 1.711659 to 74.698037 and optimal solution is HEGM-3 for Case-3 with USD 344,564,100 NPC, LCOE is USD 0.0513028/kwh and GHG emissions are 27,638,652kg/year at the optimal DOD of 10%.

The event-driven tools are advantageous in terms of real-time compression, power consumption reduction, and computing performance [56], [57]. Additionally, the assimilation of other potential optimization algorithms can enhance the performance of suggested method [58], [59]. Future research can be conducted to access the feasibility of using these tools with the recommended methodology.

5. Conclusion

It is concluded that the DOD plays a vital role in the performance of the battery. In this study, given values of DOD are investigated with the help of HOMER and the optimum value of NPC, LCOE and GHG emissions, for the HEGMs are determined. The overall cost of the energy mainly depends upon the battery's Depth of Discharge. Moreover, it is concluded that if the depth of discharge (DOD) of the battery is changed, overall cost values for the HEGMs would also be changed.

 doi:10.20944/preprints202211.0222.v1

The results concluded that Case-3 that is vanadium redox battery is the most optimal battery technology. HEGM-3 is the most optimal solution for each plant with COF ranges from 72.563919 to 74.698037 and NPC ranges from USD 205,355,000 to 430,640,400, LCOE USD 0.0513028/kwh to 0.0546779/kwh and GHG Emissions is 17,392,196 kg/year to 39,547,271 at the optimal DOD of 10, 20 and 40%.

It is achieved that DGCPC with HEGM-3 with 61.49% of NPC, 78.62% of LCOE and 84.00% of GHG emissions reduction as compared to the base model is the best cement plant.

Future cost savings can be obtained by utilizing more renewable resources. A block chain energy contract arrangement can be used as an energy transaction from these micro grids. In the smart grid structure, these micro grids can function as dispersed generators. Additional possibility is to investigate the implementation of various metaheuristic algorithms for the targeted optimization issues. The authors want to expand the study to include the effects of COVID-19 on the process industry. This study can be applied to a different ideal combination that is intended for deferred load and Big IT business. The same problem can be solved using a different algorithm, and the results can be compared to the findings of this study.

Author Contributions: Conceptualization, Y.B., S.M.Q., and A.W.; methodology, Y.B., and A.W.; implementation, Y.B; validation, S.M.Q., A.W., and F.L.; formal analysis, Y.B., S.M.Q, A.W., and F.L.; investigation, Y.B., S.M.Q., A.W., and F.L.; resources, S.M.Q., A.W., and A.A.; writing—original draft preparation, Y.B., S.M.Q., and A.W.; writing—review and editing, F.L., and A.A.; visualization, Y.B.; supervision, S.M.Q., and A.W.; project administration, S.M.Q., A.W., and A.A; funding acquisition, S.M.Q., and A.A. All authors have read and agreed to the published version of the manuscript.

Funding: No particular funding is received for this study.

Institutional Review Board Statement: Not Applicable.

Informed Consent Statement: Not Applicable.

Data Availability Statement: Not applicable.

Acknowledgments: The authors are grateful to Riphah International University Islamabad, Bahria School of Engineering and Applied Sciences, Bahria University Islamabad, and Effat University for the technical support. The authors also acknowledge financial support from the Effat University for funding this work under the Research grant number (UC#9/2June2021/7.2-21(3)5).

Conflicts of Interest: The authors declare no conflict of interest.

Abbreviation:

LA	Lead acid
Li-ion	Lithium ion
VR	Vanadium Redox
Ni-Fe	Nickle iron
MCDA	multi-criteria decision analysis
COF	Cumulative objective function
HEGMs	hybrid energy generation models
LF	load following
CC	cycle charging
DOD	depth of discharge
NPC	net present cost
LCOE	levelized cost of electricity
GHG	greenhouse gas

References

[1] A. Hussain, V.-H. Bui, and H.-M. Kim, 'Optimal sizing of battery energy storage system in a fast EV charging station considering power outages', *IEEE Trans. Transp. Electrification*, vol. 6, no. 2, pp. 453–463, 2020.

[2] X. Han *et al.*, 'A review on the key issues of the lithium ion battery degradation among the whole life cycle', *ETransportation*, vol. 1, p. 100005, 2019.

[3] I. Alsaidan, A. Khodaei, and W. Gao, 'A comprehensive battery energy storage optimal sizing model for microgrid applications', *IEEE Trans. Power Syst.*, vol. 33, no. 4, pp. 3968–3980, 2017.

[4] G. Cardoso, T. Brouhard, N. DeForest, D. Wang, M. Heleno, and L. Kotzur, 'Battery aging in multi-energy microgrid design using mixed integer linear programming', *Appl. Energy*, vol. 231, pp. 1059–1069, 2018.

[5] H. Fontenot and B. Dong, 'Modeling and control of building-integrated microgrids for optimal energy management–a review', *Appl. Energy*, vol. 254, p. 113689, 2019.

[6] M. F. Zia, E. Elbouchikhi, and M. Benbouzid, 'Optimal operational planning of scalable DC microgrid with demand response, islanding, and battery degradation cost considerations', *Appl. Energy*, vol. 237, pp. 695–707, 2019.

[7] M. Ruiz-Cortes *et al.*, 'Optimal charge/discharge scheduling of batteries in microgrids of prosumers', *IEEE Trans. Energy Convers.*, vol. 34, no. 1, pp. 468–477, 2018.

[8] F. Garcia-Torres and C. Bordons, 'Optimal economical schedule of hydrogen-based microgrids with hybrid storage using model predictive control', *IEEE Trans. Ind. Electron.*, vol. 62, no. 8, pp. 5195–5207, 2015.

[9] T. Weitzel, M. Schneider, C. H. Glock, F. Löber, and S. Rinderknecht, 'Operating a storage-augmented hybrid microgrid considering battery aging costs', *J. Clean. Prod.*, vol. 188, pp. 638–654, 2018.

[10] S. Turkdogan, 'Design and optimization of a solely renewable based hybrid energy system for residential electrical load and fuel cell electric vehicle', *Eng. Sci. Technol. Int. J.*, vol. 24, no. 2, Art. no. 2, Apr. 2021, doi: 10.1016/j.jestch.2020.08.017.

[11] S. W. Chisale and P. Mangani, 'Energy Audit and Feasibility of Solar PV Energy System: Case of a Commercial Building', *J. Energy*, vol. 2021, pp. 1–9, May 2021, doi: 10.1155/2021/5544664.

[12] Y. W. Basheer Asad; Qaisar, Saeed Mian; Ahmed, Toqeer; Ullah, Nasim; Alotaibi, Sattam, 'Analyzing the Prospect of Hybrid Energy in the Cement Industry of Pakistan, Using HOMER Pro', *Sustainability*, vol. 14, no. 19, p. 12440, 2022, doi: 10.3390/su141912440.

[13] S. Rehman, 'Hybrid power systems – Sizes, efficiencies, and economics', *Energy Explor. Exploit.*, vol. 39, no. 1, Art. no. 1, Jan. 2021, doi: 10.1177/0144598720965022.

[14] J. Li, P. Liu, and Z. Li, 'Optimal design and techno-economic analysis of a hybrid renewable energy system for off-grid power supply and hydrogen production: A case study of West China', *Chem. Eng. Res. Des.*, vol. 177, pp. 604–614, Jan. 2022, doi: 10.1016/j.cherd.2021.11.014.

[15] K. A. Kavadias and P. Triantafyllou, 'Hybrid Renewable Energy Systems' Optimisation. A Review and Extended Comparison of the Most-Used Software Tools', *Energies*, vol. 14, no. 24, Art. no. 24, Dec. 2021, doi: 10.3390/en14248268.

[16] C. Ammari, D. Belatrache, B. Touhami, and S. Makhloufi, 'Sizing, optimization, control and energy management of hybrid renewable energy system—A review', *Energy Built Environ.*, vol. 3, no. 4, pp. 399–411, Oct. 2022, doi: 10.1016/j.enbenv.2021.04.002.

[17] W. Zhu, J. Guo, and G. Zhao, 'Multi-Objective Sizing Optimization of Hybrid Renewable Energy Microgrid in a Stand-Alone Marine Context', *Electronics*, vol. 10, no. 2, Art. no. 2, Jan. 2021, doi: 10.3390/electronics10020174.

[18] F. A. Alturki, A. A. Al-Shamma'a, H. M. H. Farh, and K. AlSharabi, 'Optimal sizing of autonomous hybrid energy system using supply-demand-based optimization algorithm', *Int. J. Energy Res.*, vol. 45, no. 1, Art. no. 1, Jan. 2021, doi: 10.1002/er.5766.

[19] A. Elbaz and M. T. Güneşer, 'Optimal Sizing of a Renewable Energy Hybrid System in Libya Using Integrated Crow and Particle Swarm Algorithms', *Adv. Sci. Technol. Eng. Syst. J.*, vol. 6, no. 1, Art. no. 1, Jan. 2020, doi: 10.25046/aj060130.

[20] Y. Chen *et al.*, 'Constraint multi-objective optimal design of hybrid renewable energy system considering load characteristics', *Complex Intell. Syst.*, vol. 8, no. 2, Art. no. 2, Apr. 2022, doi: 10.1007/s40747-021-00363-4.

[21] D. Emad, M. A. El-Hameed, and A. A. El-Fergany, 'Optimal techno-economic design of hybrid PV/wind system comprising battery energy storage: Case study for a remote area', *Energy Convers. Manag.*, vol. 249, p. 114847, Dec. 2021, doi: 10.1016/j.enconman.2021.114847.

[22] Y. Cao, H. Yao, Z. Wang, K. Jermsittiparsert, and N. Yousefi, 'Optimal Designing and Synthesis of a Hybrid PV/Fuel cell/Wind System using Meta-heuristics', *Energy Rep.*, vol. 6, pp. 1353–1362, Nov. 2020, doi: 10.1016/j.egyr.2020.05.017.

[23] A. Masih and H. Verma, 'Optimum sizing and simulation of hybrid renewable energy system for remote area', *Energy Environ.*, p. 0958305X2110301, Sep. 2021, doi: 10.1177/0958305X211030112.

[24] A. Mahesh and K. S. Sandhu, 'A genetic algorithm based improved optimal sizing strategy for solar-wind-battery hybrid system using energy filter algorithm', *Front. Energy*, vol. 14, no. 1, Art. no. 1, Mar. 2020, doi: 10.1007/s11708-017-0484-4.

[25] A. S. Aziz *et al.*, 'A new optimization strategy for wind/diesel/battery hybrid energy system', *Energy*, vol. 239, p. 122458, Jan. 2022, doi: 10.1016/j.energy.2021.122458.

[26] B. N. Silva, M. Khan, and K. Han, 'Futuristic Sustainable Energy Management in Smart Environments: A Review of Peak Load Shaving and Demand Response Strategies, Challenges, and Opportunities', *Sustainability*, vol. 12, no. 14, Art. no. 14, Jul. 2020, doi: 10.3390/su12145561.

[27] V. Sidharthan Panaparambil, Y. Kashyap, and R. Vijay Castelino, 'A review on hybrid source energy management strategies for electric vehicle', *Int. J. Energy Res.*, vol. 45, no. 14, Art. no. 14, Nov. 2021, doi: 10.1002/er.7107.

[28] Sk. A. Shezan, K. N. Hasan, A. Rahman, M. Datta, and U. Datta, 'Selection of Appropriate Dispatch Strategies for Effective Planning and Operation of a Microgrid', *Energies*, vol. 14, no. 21, Art. no. 21, Nov. 2021, doi: 10.3390/en14217217.

[29] A. Aziz, M. Tajuddin, M. Adzman, M. Ramli, and S. Mekhilef, 'Energy Management and Optimization of a PV/Diesel/Battery Hybrid Energy System Using a Combined Dispatch Strategy', *Sustainability*, vol. 11, no. 3, Art. no. 3, Jan. 2019, doi: 10.3390/su11030683.

[30] V. Suresh, M. M., and R. Kiranmayi, 'Modelling and optimization of an off-grid hybrid renewable energy system for electrification in a rural areas', *Energy Rep.*, vol. 6, pp. 594–604, Nov. 2020, doi: 10.1016/j.egyr.2020.01.013.

[31] S. S. Bohra, A. Anvari-Moghaddam, F. Blaabjerg, and B. Mohammadi-Ivatloo, 'Multi-criteria planning of microgrids for rural electrification', *J. Smart Environ. Green Comput.*, 2021, doi: 10.20517/jsegc.2021.06.

[32] M. R. Elkadeem *et al.*, 'Feasibility analysis and optimization of an energy-water-heat nexus supplied by an autonomous hybrid renewable power generation system: An empirical study on airport facilities', *Desalination*, vol. 504, p. 114952, May 2021, doi: 10.1016/j.desal.2021.114952.

[33] J. O. Eko and M. C. Paul, 'Integrated Sustainable Energy for Sub-Saharan Africa: A Case Study of Machinga Boma in Malawi', *Energies*, vol. 14, no. 19, Art. no. 19, Oct. 2021, doi: 10.3390/en14196330.

[34] J. O. Oladigbolu, M. A. M. Ramli, and Y. A. Al-Turki, 'Feasibility Study and Comparative Analysis of Hybrid Renewable Power System for off-Grid Rural Electrification in a Typical Remote Village Located in Nigeria', *IEEE Access*, vol. 8, pp. 171643–171663, 2020, doi: 10.1109/ACCESS.2020.3024676.

[35] J. J. D. Nesamalar, S. Suruthi, S. C. Raja, and K. Tamilarasu, 'Techno-economic analysis of both on-grid and off-grid hybrid energy system with sensitivity analysis for an educational institution', *Energy Convers. Manag.*, vol. 239, p. 114188, Jul. 2021, doi: 10.1016/j.enconman.2021.114188.

[36] C. Malanda, A. B. Makokha, C. Nzila, and C. Zalengera, 'Techno-economic optimization of hybrid renewable electrification systems for Malawi's rural villages', *Cogent Eng.*, vol. 8, no. 1, Art. no. 1, Jan. 2021, doi: 10.1080/23311916.2021.1910112.

[37] H. Rezk, M. Al-Dhaifallah, Y. B. Hassan, and H. A. Ziedan, 'Optimization and Energy Management of Hybrid Photovoltaic-Diesel-Battery System to Pump and Desalinate Water at Isolated Regions', *IEEE Access*, vol. 8, pp. 102512–102529, 2020, doi: 10.1109/ACCESS.2020.2998720.

[38] S. A. Sadat, J. Faraji, M. Babaei, and A. Ketabi, 'Techno-economic comparative study of hybrid microgrids in eight climate zones of Iran', *Energy Sci. Eng.*, vol. 8, no. 9, Art. no. 9, Sep. 2020, doi: 10.1002/ese3.720.

[39] N. Majdi Nasab, J. Kilby, and L. Bakhtiaryfard, 'Case Study of a Hybrid Wind and Tidal Turbines System with a Microgrid for Power Supply to a Remote Off-Grid Community in New Zealand', *Energies*, vol. 14, no. 12, Art. no. 12, Jun. 2021, doi: 10.3390/en14123636.

[40] J. H. Peterseim, S. White, A. Tadros, and U. Hellwig, 'Concentrating solar power hybrid plants – Enabling cost effective synergies', *Renew. Energy*, vol. 67, pp. 178–185, Jul. 2014, doi: 10.1016/j.renene.2013.11.037.

[41] A. Lajunen, 'Energy consumption and cost-benefit analysis of hybrid and electric city buses', *Transp. Res. Part C Emerg. Technol.*, vol. 38, pp. 1–15, Jan. 2014, doi: 10.1016/j.trc.2013.10.008.

[42] M. D. A. Al-falahi, S. D. G. Jayasinghe, and H. Enshaei, 'A review on recent size optimization methodologies for standalone solar and wind hybrid renewable energy system', *Energy Convers. Manag.*, vol. 143, pp. 252–274, Jul. 2017, doi: 10.1016/j.enconman.2017.04.019.

[43] Y. Sawle, S. C. Gupta, and A. K. Bohre, 'Review of hybrid renewable energy systems with comparative analysis of off-grid hybrid system', *Renew. Sustain. Energy Rev.*, vol. 81, pp. 2217–2235, Jan. 2018, doi: 10.1016/j.rser.2017.06.033.

[44] I. P. Panapakidis, D. N. Sarafianos, and M. C. Alexiadis, 'Comparative analysis of different grid-independent hybrid power generation systems for a residential load', *Renew. Sustain. Energy Rev.*, vol. 16, no. 1, pp. 551–563, Jan. 2012, doi: 10.1016/j.rser.2011.08.021.

[45] J. I. Lewis and R. H. Wiser, 'Fostering a renewable energy technology industry: An international comparison of wind industry policy support mechanisms', *Energy Policy*, vol. 35, no. 3, pp. 1844–1857, Mar. 2007, doi: 10.1016/j.enpol.2006.06.005.

[46] 'Pro, H. Homer Pro'. https://www.homerenergy.com/products/pro/docs/latest/index.html (accessed Oct. 30, 2022).

[47] Sk. A. Shezan *et al.*, 'Effective dispatch strategies assortment according to the effect of the operation for an islanded hybrid microgrid', *Energy Convers. Manag. X*, vol. 14, p. 100192, May 2022, doi: 10.1016/j.ecmx.2022.100192.

[48] D. Icaza-Alvarez, F. Jurado, M. Tostado-Véliz, and P. Arevalo, 'Design to include a wind turbine and socio-techno-economic analysis of an isolated airplane-type organic building based on a photovoltaic/hydrokinetic/battery', *Energy Convers. Manag. X*, vol. 14, p. 100202, May 2022, doi: 10.1016/j.ecmx.2022.100202.

[49] Y. B. Muna and C.-C. Kuo, 'Feasibility and Techno-Economic Analysis of Electric Vehicle Charging of PV/Wind/Diesel/Battery Hybrid Energy System with Different Battery Technology', *Energies*, vol. 15, no. 12, p. 4364, Jun. 2022, doi: 10.3390/en15124364.

[50] S. Barakat, A. Emam, and M. M. Samy, 'Investigating grid-connected green power systems' energy storage solutions in the event of frequent blackouts', *Energy Rep.*, vol. 8, pp. 5177–5191, Nov. 2022, doi: 10.1016/j.egyr.2022.03.201.

[51] V. J. Prakash and P. K. Dhal, 'Techno-Economic Assessment of a Standalone Hybrid System Using Various Solar Tracking Systems for Kalpeni Island, India', *Energies*, vol. 14, no. 24, p. 8533, Dec. 2021, doi: 10.3390/en14248533.

[52] R. Zieba Falama *et al.*, 'A comparative study based on a techno-environmental-economic analysis of some hybrid grid-connected systems operating under electricity blackouts: A case study in Cameroon', *Energy Convers. Manag.*, vol. 251, p. 114935, Jan. 2022, doi: 10.1016/j.enconman.2021.114935.

[53] M. Ur Rashid, I. Ullah, M. Mehran, M. N. R. Baharom, and F. Khan, 'Techno-Economic Analysis of Grid-Connected Hybrid Renewable Energy System for Remote Areas Electrification Using Homer Pro', *J. Electr. Eng. Technol.*, vol. 17, no. 2, pp. 981–997, Mar. 2022, doi: 10.1007/s42835-021-00984-2.

[54] 'Nepra (2022) Industrial Tariff', Oct. 02, 2022. https://nepra.org.pk/consumer%20affairs/Electricity%20Bill.php

[55] 'Global Solar Atlas, Globalsolaratlas.info', 2021. https://globalsolaratlas.info/map

[56]Mian Qaisar, S., 'Event-driven coulomb counting for effective online approximation of Li-ion battery state of charge', Energies, vol. 13, no. 21, 2020, doi: 10.3390/en13215600.

[57] Qaisar, S. M., Khan, S. I., Dallet, D., Tadeusiewicz, R., & Pławiak, P., 'Signal-piloted processing metaheuristic optimization and wavelet decomposition based elucidation of arrhythmia for mobile healthcare', Biocybernetics and Biomedical Engineering, vol. 42, no. 2, 2022, pp. 681-694, doi: 10.1016/j.bbe.2022.05.006.

[58] Qaisar, S. M., Khan, S. I., Srinivasan, K., & Krichen, M., 'Arrhythmia classification using multirate processing metaheuristic optimization and variational mode decomposition', Journal of King Saud University-Computer and Information Sciences, 2022, doi: 10.1016/j.jksuci.2022.05.009.

[59] Abbas, A., Qaisar, S. M., Waqar, A., Ullah, N., & Al Ahmadi, A. A., 'Min-Max Regret-Based Approach for Sizing and Placement of DGs in Distribution System under a 24 h Load Horizon', Energies, vol. 15, no. 10, 2022, doi: 10.3390/en15103701.